ACS Medicinal Chemistry Letters

Letter

Discovery of Selective, Orally Bioavailable Pyrazolopyridine Inhibitors of Protein Kinase C# (PKC#) that Ameliorate Symptoms of Experimental Autoimmune Encephalomyelitis

Philip N Collier, Heather C. Twin, Ronald M. A. Knegtel, Dean Boyall, Guy Brenchley, Christopher J. Davis, Shazia Keily, Chau Mak, Andrew Miller, Françoise Pierard, Luca Settimo, Clare M. Bolton, Peter Chiu, Adam Curnock, Elisabeth Doyle, Adam J Tanner, and Juan-Miguel Jimenez

ACS Med. Chem. Lett., **Just Accepted Manuscript** • DOI: 10.1021/acsmedchemlett.9b00134 • Publication Date (Web): 27 Jun 2019

Just Accepted

is published by the American Chemical Society. 1155 Sixteenth Street N.W., Washington, DC 20036

Discovery of Selective, Orally Bioavailable Pyrazolopyridine Inhibitors of Protein Kinase Cθ (PKCθ) that Ameliorate Symptoms of Experimental Autoimmune Encephalomyelitis

Philip N. Collier,*† Heather C. Twin,* Ronald M. A. Knegtel, Dean Boyall, Guy Brenchley, Christopher J. Davis, Shazia Keily, Chau Mak, Andrew Miller, Françoise Pierard, Luca Settimo, Clare M. Bolton, Peter Chiu, Adam Curnock, Elisabeth Doyle,† Adam J. Tanner, Juan-Miguel Jimenez

Vertex Pharmaceuticals (Europe) Ltd., 86-88 Jubilee Avenue, Milton Park, Abingdon OX14 4RW, United Kingdom

†Vertex Pharmaceuticals Inc., 50 Northern Avenue, Boston, Massachusetts 02210, United States

KEYWORDS. PKCθ, multiple sclerosis, kinases, oxetane.

ABSTRACT: PKCθ plays an important role in T cell biology and is a validated target for a number of disease states. A series of potent and selective PKCθ inhibitors were designed and synthesized starting from a HTS hit compound. Cell activity, while initially a challenge to achieve, was built into the series by transforming the nitrile unit of the scaffold into a primary amine, the latter predicted to form a new hydrogen bond to Asp508 near the entrance of the ATP binding site of PKCθ. Significant improvements in physiochemical parameters were observed on introduction of an oxetane group proximal to a primary amine leading to compound **22**, which demonstrated a reduction of symptoms in a mouse model of multiple sclerosis.

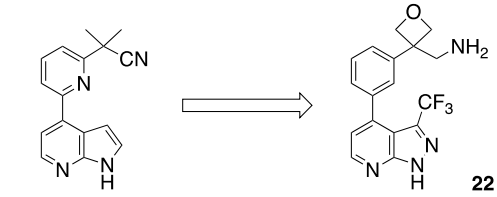

PKCθ Ki = 3 nM
IL-2 IC_{50} = 2.6 μM

PKCθ Ki = 6 nM
IL-2 IC_{50} = 0.19 μM
Efficacy in murine EAE

Protein kinase C (PKC) are a large family of serine/threonine kinases that are involved in the regulation of a number of essential cellular processes. The family consists of 11 PKC isoforms that are separated into 3 different classes: (i) diacylglycerol (DAG) and calcium dependent classical isoforms (PKCs α, βI, βII, and γ); (ii) DAG-dependent novel isoforms (PKCs δ, ε, η, and θ); (iii) DAG and calcium independent atypical isoforms (PKCs λ, ι, and ζ).[1] PKCθ, one of the novel PKC isoforms, mediates an immune response *via* T-cell activation, differentiation and migration and is the only member of the PKC family known to translocate to the immunological synapse.[2]

PKCθ is mainly expressed in T lymphocytes and the phenotype of the knockout mouse implies a central role in T-cell activation by integrating signals from both the T cell receptor (TCR) and the co-stimulatory CD28.[3,4] PKCθ appears to be important for the development of T cell mediated inflammatory diseases, because PKCθ-deficient mice display resistance in models of asthma[5] and IBD,[6] collagen-induced arthritis (CIA),[7] and experimental autoimmune encephalomyelitis (EAE), a commonly used model of multiple sclerosis (MS).[8,9] PKCθ-deficient mice however, are able to mount normal T-cell responses to certain pathogens, and anti-viral responses seem to remain intact.[10-12] In addition to the unique role that PKCθ plays in T-cell activation, inhibition of PKCθ enhances Treg function.[13] PKCθ inhibition may be a useful approach towards treating T-cell-mediated inflammatory diseases such as rheumatoid arthritis, inflammatory bowel disease and psoriasis, by inhibiting T-cell activation and enhancing Treg function, without leading to broad immunosuppression.

Despite the PKC family being the focus of research over the past two decades,[14,15] a selective PKCθ inhibitor has yet to reach the clinic.[16-18] The catalytic domain is highly conserved among the different isoforms thus making the design of selective inhibitors challenging.[19] Sotrastaurin (AEB071),[20] a pan-PKC inhibitor developed by Novartis, inhibits T-cell activation via PKC by the binding of peptide-MHC complexes and CD28 co-stimulation.[21] Sotrastaurin displays poor kinome selectivity, inhibiting more than 200 other kinases, including those important for early T-cell activation such as Lck. A transient increase in heart rate has been observed in clinical trials with Sotrastaurin, leading to questions around the feasibility of developing a safer approach through selective inhibition of one PKC isoform instead of multiple PKC isoforms.[22,23] Selective PKCθ inhibition is postulated to provide a better balance of efficacy and safety.

In 2015, AbbVie published their efforts towards the discovery of selective PKC theta inhibitors.[24,25] An advanced lead compound displayed efficacy in a mouse model of arthritis but was poorly tolerated at doses marginally higher than the efficacious dose. Further efforts focused on improving tolerability, led to compounds that, despite good exposure, yielded only moderate efficacy in a chronic in vivo mouse model of arthritis.

As part of our own program to identify potent and selective PKCθ inhibitors,[26-28] biochemical screening of the Vertex compound collection led to the identification of **1** as a suitable starting point for medicinal chemistry optimization efforts (Table 1). It displayed high affinity for inhibition of PKCθ and possessed drug-like properties (MW 262, clogP 2, PSA 65 Å^2). Compound **1** showed some isoform selectivity against PKCα but minimal selectivity against PKCδ, an enzyme deemed necessary to avoid because of the risk of B-cell autoimmunity associated with its inhibition. It also showed strong activity against a range of other kinases (e.g. K_i: PKA, 110 nM; GSK-3β, 210 nM; ROCK, 6 nM; JAK-3, 3 nM; FLT-3, 100 nM). Poor rat hepatocyte stability resulted in high clearance when **1** was dosed intravenously in rat.

Initial optimization work led to improvements in general kinase selectivity as a result of transitioning from a 1*H*-pyrrolo[2,3-*b*]pyridine to a 1*H*-pyrazolo[3,4-*b*]pyridine core (Table 1). The selectivity improvements observed with **2** and **3** are likely due to the presence of Thr442, located directly underneath the pyrazolopyridine 2-position nitrogen atom, being replaced by a more lipophilic valine in other kinases like ROCK, PKA and JAK2. These modifications also led to improved rat metabolic stability and lower *in-vivo* clearance. The improved rat hepatocyte stability of **2** compared to **1**, correlates with a lower lipophilicity ($logD_{7.4}$ of **1**, 3.4; of **2**, 2.9).

TABLE 1. Early Optimization of HTS Hit Compound 1.

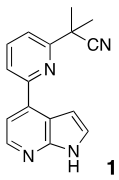

1

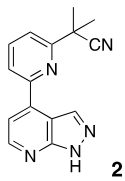

2

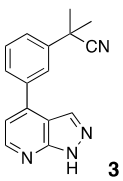

3

Cpd[a]	PKCθ	PKC α, δ	ROCK, JAK2	Cl/Fu (R/H)[b]	Rat iv PK[c] Cl, $T_{1/2}$, V_{ss}
1	3	110, 12	6, 13	156, 24	42, 0.3, 0.99
2	14	465, 240	210, 86	24, 33	22, 2.5, 1.22
3	28	ND, 584	560, 270	58, 172	12, 4.6, 0.94

[a]All enzyme data are Ki and expressed in nM. [b]Unbound Hep Cl expressed in µL/min/10^{6}cells. [c]CL expressed in mL/min/Kg, $T_{1/2}$ in h and V_{ss} in L/Kg.

Compound **1** was docked in a published crystal structure of PKCθ as described previously.[27] In the resulting model, the cyano moiety sits in a small hydrophobic pocket under the glycine-rich loop (GRL) (Figure 1). Opportunities for obtaining selectivity over PKC isoforms were identified by comparing the model of compound **1** bound to PKCθ with homology models of other PKC isoforms built using PKCθ as a structural template. Within the C-terminus there is a significant sequence difference between the PKC isoforms, involving the replacement of the relatively small Cys661 in PKCθ with much larger residues such as Tyr630 in PKCδ (Figure 1). As a consequence of this residue difference, a larger hydrophobic pocket, delineated by Phe664 (C-terminus) and Leu386 (GRL), is accessible in PKCθ as compared to other PKCs. This area of the ATP binding site could be further explored to gain both potency and selectivity.

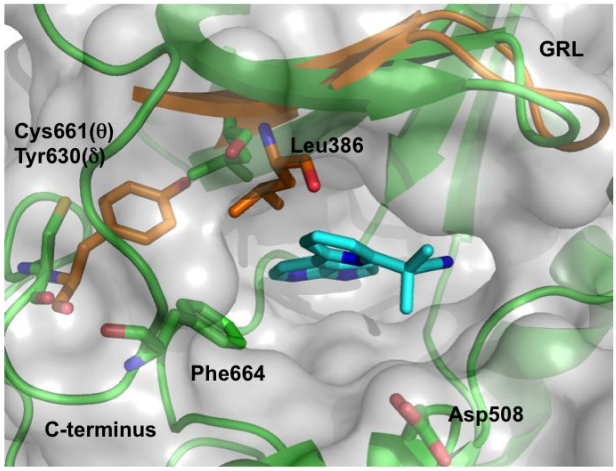

Figure 1. Predicted binding mode of **1** (cyan) in PKCθ (grey/green). The cyano group points into a small hydrophobic pocket under the glycine-rich loop (GRL). The replacement of the smaller Cys661 in PKCθ with the larger Tyr630 in PKCδ (brown) in the C-terminus results in the presence of a larger hydrophobic pocket in PKCθ located between Phe664 (C-terminus) and Leu386 (GRL)

Based on the above modeling, a range of α,α-disubstituted nitriles were designed and synthesized, all possessing nanomolar biochemical affinity (data not reported). However, none of these compounds or the ones reported earlier in the manuscript had sub-micromolar cell potency for the inhibition of IL-2 release from PBMCs following stimulation with anti-CD3/CD28. It was confirmed that poor cell permeability was not the reason behind the observed weak cell potency (Caco-2 data for compound **2**: A-B = 20.1 x 10^{-6} cm/s, E.R. = 0.95;

compound **3**: A-B: 36 x 10^{-6} cm/s, E.R. = 0.7). A breakthrough in this area came when the nitriles were converted into the corresponding primary amines (Table 2, **5 - 11**).

Molecular modeling studies suggested a different binding mode of amine **6** in PKCθ compared to nitrile **4** (Table 2). When docked into PKCθ, the primary amine of **6** projects towards solvent, unlike the nitrile group of **4** which projects under the glycine-rich loop. This change in positioning of the polar functionality is driven by a predicted hydrogen bond involving the amine of **6** and the backbone carbonyl of Asp508 as well as favorable electrostatic interactions with the carboxylate groups of aspartates 465 and 508 as shown in Figure 2.

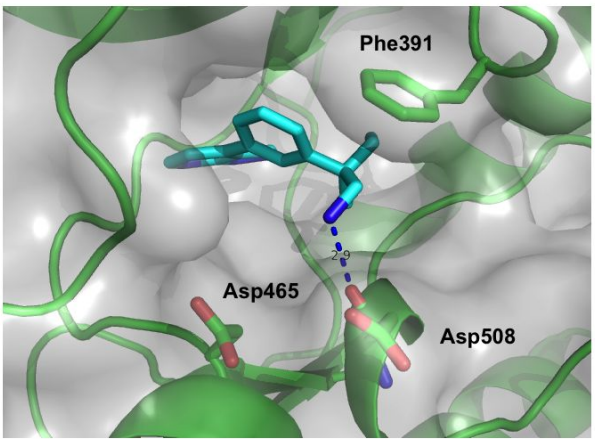

Figure 2. Predicted binding mode of **6** in the active site of PKCθ. Compound **6** is coloured cyan and PKCθ is depicted in grey/green. Key amino acid side chains are labeled and depicted as sticks.

Cell potency could be modulated by varying the substituents at the benzylic position of the scaffold (Table 2). Modeling suggests that the highly potent alkyne **7** extends further into the back of the active site and fills the same pocket occupied by the cyano group of **4**, and the ethyl group of **6** (Figure 3A). In our model, the alkyne moiety fits tightly into this pocket and is in van der Waals contact with the gatekeeper reside Met458 while engaging in aromatic stacking interactions with Phe391 of the GRL.

Binding of the increasingly large alkyl rings of compounds **8-10** requires conformational adjustments of both the inhibitor and the kinase GRL/C-terminus. Only in PKCθ can both of these adjustments readily be accommodated because there is more space available between the C-terminus and the GRL. This is because the residue equivalent to Cys661 in the C-terminus of PKCθ is a larger tyrosine or leucine in PKCδ and PKCα, respectively. With the introduction of an ether oxygen in the THP ring of compound **11**, modeling suggests that the inhibitor becomes fixed in space by two hydrogen bonds involving the salt-bridge Lys409 and the backbone carbonyl of Asp508 (Figure 3B). With the inhibitor fixed by hydrogen bonding, the binding of large rings now solely depends on the ability of the GRL and C-terminus to accommodate them. The improved selectivity profile of **11** is therefore likely due to PKCθ having more space available near its GRL/C-terminus interface compared to other PKC sub-types with larger residues in their C-termini.

Table 2. SAR exploration of scaffold benzylic position

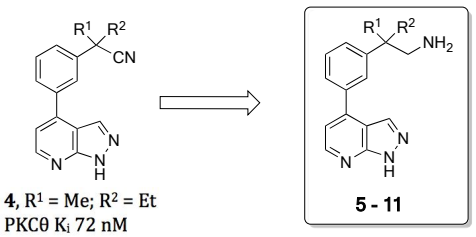

4, R^1 = Me; R^2 = Et
PKCθ K_i 72 nM
IL-2 IC_{50} 2.7 μM

Cpd	R^1, R^2	PKCθ Ki[a]	PKCδ / PKCθ	PKCα / PKCθ	IL-2 IC_{50}[b]
5	Me, Me	12	16	50	0.33
6	Me, Et	3	13	37	0.17
7	Me, CH_2CCH	0.2	36	149	0.02
8	$-(CH_2)_3-$	17	18	41	0.30
9	$-(CH_2)_4-$	22	18	28	0.35
10	$-(CH_2)_5-$	30	8	18	0.58
11	$-(CH_2)_2O(CH_2)_2-$	9	111	93	0.55

[a]Enzyme Ki are expressed in nM. [b]Cell IC_{50} are expressed in μM.

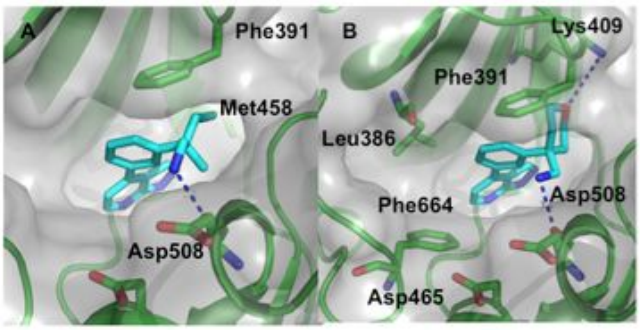

Figure 3. (A) Predicted binding pose of **7** in PKCθ; (B) Predicted binding mode of **11** in PKCθ. Inhibitors are coloured cyan and PKCθ grey/green, key amino acid side chains are labeled and depicted as sticks.

Selectivity over PKCδ could be improved by targeting the C-terminus region *via* meta-substitution on the central benzene ring (Table 3). As shown in Figure 1, the meta position projects substituents towards a hydrophobic pocket located between Phe664 (C-terminus) and Leu386 (GRL). Alkyl substituted compounds **12-14** improved selectivity over PKCδ by occupying a pocket that is slightly larger in PKCθ compared to PKCδ due to the Cys661/Tyr630 sequence difference in the C-terminus.

Table 3. SAR exploration of meta position of benzene ring

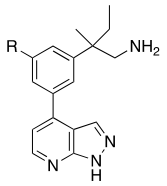

6, 12 - 14

Cpd	R	PKCθ Ki[a]	PKCδ / PKCθ	IL-2 IC_{50}[b]
6	H	3	14	0.17
12	Me	5	24	0.26
13	Et	14	39	0.25
14	Pr	32	39	0.2

[a]Enzyme Ki are expressed in nM. [b]Cell IC_{50} are expressed in μM.

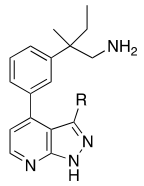

6, 15 - 17

Cpd	R	PKCθ Ki[a]	PKCδ / PKCθ	IL-2 IC_{50}[b]
6	H	2	24	0.17
15	Me	<1	>16	0.10
16	Cl	0.3	22	0.02
17	CF_3	0.4	25	0.01

[a]Enzyme Ki are expressed in nM. [b]Cell IC_{50} are expressed in μM.

Substitution at the C3-position of the pyrazolopyridine core led to increased PKCθ affinity. For example, substitution with a 3-trifluoromethyl group improved cell potency ten-fold, while maintaining a reasonable PK profile (**17**, rat IV PK: CL = 45 ml/min/kg; $T_{1/2}$ = 1.8 h; Vss = 2.7). As the central phenyl ring is already rotated out of the plane of the azaindazole ring system by ~40º due to steric hindrance with the pyrazole ring, substitution on the 3-position only has a small effect on the overall conformation of the inhibitor. The observed gain in potency is presumably due to the substituent on the 3-position occupying a small hydrophobic pocket positioned in between the ligand's central phenyl ring and the Met458 gatekeeper residue of PKCθ (Figure 4).

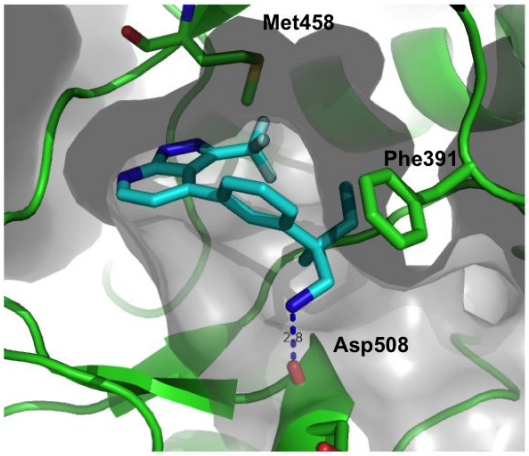

Figure 4. Predicted binding pose of **17** in PKCθ. The inhibitor is colored cyan and PKCθ grey/green, key amino acid side chains are labeled and depicted as sticks.

Table 4. SAR exploration of pyrazolopyridine C3-position

The knowledge generated from the above SAR studies led to the preparation of advanced lead compounds **18-22 (**Table 5**)**. Cyclobutanes **18** and **19** potently inhibited PKCθ and secretion of IL-2 from stimulated PBMCs, and were isoform selective against PKCα and δ. However, they strongly inhibited the hERG ion channel, raising safety concerns. THP compound **20** was also prepared and showed reduced activity at the hERG ion channel. THP analogs such as **20** were deprioritized however, due to their cross activity against other kinases (e.g. PKA and FLT-3 Ki values, 30 and 46 nM respectively).

In order to further build on the improved profile observed with THP analog **20**, oxetane-containing compounds **21** and **22**, were prepared. It has been established that the introduction of the oxetane unit onto molecular scaffolds can have a profound impact on physiochemical properties such as lipophilicity, metabolic stability and aqueous solubility.[29] Although **21** and **22** displayed reduced biochemical and cellular activities, they led to improved isoform selectivity profiles compared to **20**. **21** and **22** showed improved CYP450 inhibition profiles (**21**: 22, >30, >30 μM vs. **18**: 16, 4, 8 μM against CYP3A4, 2C9, 2D6 respectively) and generally increased metabolic stability compared to the corresponding cyclobutanes **18** and **19**, correlating with lower logD (experimental values for **18**, **21, 22**: 2.9, 2.2 and 1.7 respectively). Lower hERG affinities were observed for oxetane amines **21** and **22**, when compared to cyclobutylamines **18** and **19**, perhaps reflective of the lower basicity of the former (pKa: 7.9 and 7.6 for **21** and **22** respectively vs. 8.8 and 8.8 for **18** and **19** respectively). Cyclobutane **19** and tetrahydropyran **20** showed cytotoxicity at a significantly lower concentration than oxetane **22** in a HFL-1 counter-screening assay measuring inhibition of cell growth.

Oxetane **22** was chosen for further characterization *in vitro* and *in vivo* on the basis of it possessing the most balanced overall profile. **22** showed good selectivity when profiled against a wide panel of kinases (inhibiting 2/49 kinases >50% at 0.4 μM, see Supporting Information) and a non-kinase panel of receptors and ion-channels (>50% inhibition at 10 μM for 2/68). **22** was permeable and showed no significant efflux (Caco-2 A-B = 19, ER 2.4). On intravenous (i.v.) administration, compound **22** displayed high clearance (62 mL/min/Kg) and short half-life (1.2 h) in rat, but much lower clearance and longer half-lives in higher species (clearance of

12 and 9 mL/min/Kg in dog and cynomolgus monkeys respectively; corresponding $T_{1/2}$ = 6.2 and 5.1 h respectively). **22** showed moderate to good bioavailability when dosed orally in mouse (67%) and rat (46%) and displayed good thermodynamic solubility (515 μM). This overall PK profile suggested that exposure of **22** would be sufficient to modulate PKCθ in an in-vivo model. Indeed, we demonstrated that **22** significantly inhibits IL-2 as part of an assessment of IL-2 production in vivo (see Supporting Information). Furthermore, we found that unbound brain exposure 3h post po dose was comparable (0.19 uM @ 50 mg/kg) or exceeded (0.4 uM @ 100 mg/kg) IL-2 IC_{50} of 0.2 uM, indicating ample target coverage.

We also wanted to assess if compound **22** showed activity against the Th17 subset of CD^+ T-cells. There is strong evidence that Th17 cells mediate the autoimmune inflammation and tissue damage in MS by the release of pro-inflammatory cytokines such as IL-17, IL-21 and IL-22. These cells have been found to be present in both the CNS and immune periphery in the EAE mouse model and have been detected in the brain tissues of patients with MS.[30] **22** inhibited the release of IL-17 from CD3/CD28 stimulated Th-17 cells with an IC_{50} of 1 μM.

Table 5. Profiles of advanced lead compounds 18-22

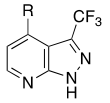

18 - 22

R	PKCθ, δ, α Ki[a]	IL-2 IC_{50}[b]	HFL-1 IC_{50}[b]	RLM, HLM[c]	hERG[d]
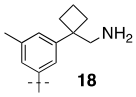 **18**	3, 135, 60	0.06	0.65	56, 81	0.7
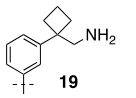 **19**	2, 60, 57	0.09	1.9	88, 81	3
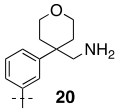 **20**	9, 184, 468	0.13	3.3	65, 96	>10
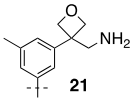 **21**	8, 542, 286	0.45	2.5	59, 86	>10
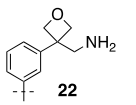 **22**	6, 392, 1020	0.21	>10	77, 100	>10

[a]Enzyme Ki are expressed in nM. [b]Cell IC_{50} are expressed in μM. [c]% remaining @ 30 min; [d]IC_{50} and expressed in μM.

Compound **22** was evaluated in murine experimental autoimmune encephalomyelitis (EAE), a well-established model of MS. Two previous studies have genetically validated PKCθ in EAE.[8,9] PKCθ knock out mice treated with MOG antigen were resistant to EAE, the resistance reported to be due to decreased cytokine production by T cells and failure of these cells to penetrate into the CNS. Our group has previously reported on the pharmacological validation of PKCθ in EAE.[28]

In this experiment, C57BL6 mice were immunized with MOG antigen and allowed to develop symptoms of EAE. Animals were dosed with vehicle, or **22**, on reaching a clinical score of 1-1.5. We found that therapeutic dosing of **22** at 50 mg/kg was effective in reducing symptoms in animals with ongoing disease (Figure 5). A recent publication described the amelioration of clinical symptoms of EAE with PKCβ inhibitor LY-317615 via stabilization of blood-brain barrier disruption.[31] We confirmed that the efficacy we observed with **22** in EAE was not due to inhibition of the PKCβ isozyme, (Ki = 1.7 μM for **22**).

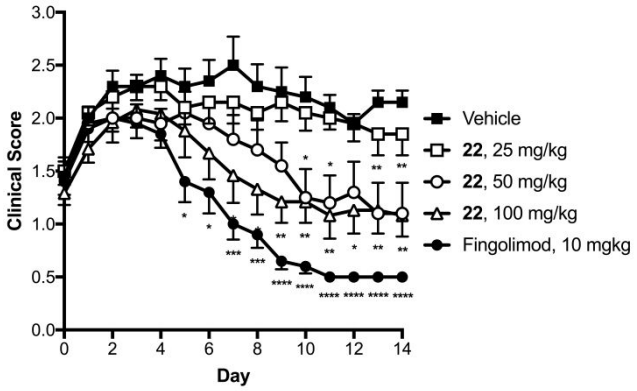

Figure 5. Therapeutic dosing of **22** in MOG EAE mouse model. Please see Supporting Information for statistical analysis of these EAE data.

In summary, we have discovered a series of selective inhibitors of PKCθ starting from a promiscuous HTS hit compound, using structural information to guide design. Transforming a nitrile moiety on the scaffold into a primary amine led to a serendipitous and large increase in cell activity. Optimization of in vitro ADMET properties was achieved by incorporating an oxetane motif adjacent to a primary amine. Efficacy of **22** in mouse EAE validates our mechanistic hypothesis that modulation of PKCθ in vivo has potential for the treatment of MS.

ASSOCIATED CONTENT

Supporting Information

The Supporting Information is available free of charge on the ACS Publications website.

Molecular formula strings (CSV)

Chemistry and synthetic schemes, synthetic procedures and compound characterization, description of biochemical assays, description of cellular assays, molecular modeling, EAE model, physiochemical properties and DMPK assays (PDF)

AUTHOR INFORMATION

Corresponding Author

*Email: philip_collier@vrtx.com. Phone: +1 (617) 341-6921.
*Email: heather_twin@vrtx.com. Phone: + 44 (12) 35438826.

Author Contributions

All authors have given approval to the final version of the manuscript.

ACKNOWLEDGMENT

The authors thank Dr. Barry Davis for assistance in collecting some experimental data.

ABBREVIATIONS

ADMET, absorption, distribution, metabolism, excretion and toxicity; HFL-1, human fibroblast cell line-1; HTS, high throughput screening; IL-2, interleukin-2.

REFERENCES

(1) Rosse, C.; Linch, M.; Kermorgant, S.; Cameron, A. J.; Boeckeler, K.; Parker, P. J. PKC and the control of localized signal dynamics. *Nat. Rev. Mol. Cell Biol.* **2010**, *11*, 103–112.

(2) Zanin-Zhorov, A.; Dustin, M.L; Blazar, B.R. PKCtheta function at the immunological synapse: prospects for therapeutic targeting *Trends Immun*. **2011**, *32*, 358–363.

(3) Sun, Z.; Arendt, C. W.; Ellmeier, W.; Schaeffer, E. M.; Sunshine, M. J.; Gandhi, L.; Annes, J.; Petrzilka, D.; Kupfer, A.; Schwartzberg, P. L.; Littman, D. R. PKC-theta is required for TCR-induced NF-kappaB activation in mature but not immature T lymphocytes. *Nature* **2000**, *404*, 402–407.

(4) Pfeifhofer, C.; Kofler, K.; Gruber, T.; Tabrizi, N. G.; Lutz, C.; Maly, K.; Leitges, M.; Baier, G. Protein kinase C theta affects Ca2+ mobilization and NFAT cell activation in primary mouse T cells. *J. Exp. Med.* **2003**, *197*, 1525–1535.

(5) Salek-Ardakani, S.; So, T.; Halteman, B. S.; Altman, A.; Croft, M. Differential regulation of Th2 and Th1 lung inflammatory responses by protein kinase C theta. *J. Immunol*. **2004**, *173*, 6440–6447.

(6) Nagahama, K.; Ogawa, A.; Shirane, K.; Shimomura, Y.; Sugimoto, K.; Mizoguchi, A. Protein kinase C theta plays a fundamental role in different types of chronic colitis. *Gastroent*. **2008**, *134*, 459–469.

(7) Healy, A. M.; Izmailova, E.; Fitzgerald, M.; Walker, R.; Hattersley, M.; Silva, M.; Siebert, E.; Terkelsen, J.; Picarella, D.; Pickard, M. D.; LeClair, B.; Chandra, S.; Jaffee, B. PKC-theta-deficient mice are protected from Th1-dependent antigen-induced arthritis. *J. Immunol.* **2006**, *177*, 1886–1893.

(8) Tan, S.-L.; Zhao, J.; Bi, C.; Chen, X. C.; Hepburn, D. L.; Wang, J.; Sedgwick, J. D.; Chintalacharuvu, S. R.; Na, S. Resistance to experimental autoimmune encephalomyelitis and impaired IL-17 production in protein kinase C theta-deficient mice. *J. Immunol*. **2006**, *176*, 2872–2879.

(9) Salek-Ardakani, S,; So, T.; Halteman, B. S.; Altman, A.; Croft, M. Protein kinase Cθ controls Th1 cells in experimental autoimmune encephalomyelitis. *J. Immunol*. **2005**, *175*, 7635–7641.

(10) Marsland, B.J.; Soos, T.J.; Spath, G.; Littman, D.R.; Kopf, M. Protein kinase Cθ is critical for the development of in vivo T helper (Th)2 cell but not Th1 cell responses. *J. Exp. Med.* **2004**, *200*, 181–189.

(11) Giannoni, F.; Lyon, A.B.; Wareing, M.D.; Dias, P.B.; Sarawar, S.R. Protein kinase Cθ is not essential for T-cell-mediated clearance of murine gamma herpes virus 68. *J. Virol.* **2005**, *79*, 6808–6813.

(12) Marsland, B.J.; Nembrini, C.; Schmitz, N.; Abel, B.; Krautwald, S.; Bachmann, M.F.; Kopf, M. Innate signals compensate for the absence of PKC-θ during in vivo CD8+ T cell effector and memory responses. *Proc. Natl. Acad. Sci. U. S. A.* **2005**, *102*, 14374–14379.

(13) Zanin-Zhorov, A.; Ding, Y.; Kumari, S.; Attur, M.; Hippen, K. L.; Brown, M.; Blazar, B. R.; Abramson, S. B.; Lafaille, J. J.; Dustin, M. L. Protein kinase C-theta mediates negative feedback on regulatory T cell function. *Science* **2010**, *328*, 372–376.

(14) Mochly-Rosen, D.; Das, K.; Grimes, K.V. Protein kinase C, an elusive therapeutic target? *Nat. Rev. Drug Disc.* **2012**, *11*, 937–957.

(15) Chand, S.; Mehta, N.; Bahia, M. S.; Dixit, A.; Silakari, O. Protein kinase C-theta inhibitors: A novel therapy for inflammatory disorders. *Curr. Pharm. Des.* **2012**, *18*, 4725–4746.

(16) Boschelli, D. H. Small molecule inhibitors of PKC Theta as potential antiinflammatory therapeutics. *Curr. Top. Med. Chem*. **2009**, *9*, 640–654.

(17) Kunikawa, S.; Tanaka, A.; Mukoyoshi, K.; Nagashima, S.; Tominaga, H.; Chida. N.; Tasaki, M.; Shirai, F. Optimization of 2,4-diamino-5-fluoropyrimidine derivatives as protein kinase C theta inhibitors with mitigated time-dependent drug-drug interactions and P-gp liability. *Bioorg. Med. Chem*. **2015**, *23*, 3269.

(18) Fukahori, H; Chida, N.; Maeda, M.; Tasaki, M.; Kawashima, T.; Matsuoka, H.; Suzuki, K.; Ishikawa, T.; Tanaka, A.; Higashi, Y. Effect of AS2521780, a novel PKCθ selective inhibitor on T cell-mediated immunity. *Eur. J. Pharm*. **2014**, *745*, 217–222.

(19) Hage-Sleiman, R.; Hamze, A.B.; Reslan, L.; Kobeissy, H.; Dbaibo, G. The novel PKC theta from benchtop to clinic. *J. Immun. Res.* **2015**, 1–16.

(20) Wagner, J.; von Matt, P.; Sedrani, R.; Albert, R.; Cooke, N.; Ehrhardt, C.; Geiser, M.; Rummel, G.; Stark, W.; Strauss, A.; Cowan-Jacob, S. W.; Beerli, C.; Weckbecker, G.; Evenou, J. P.; Zenke, G.; Cottens, S. Discovery of 3-(1H-indol-3-yl)-4-[2-(4-methylpiperazin-1-yl)quinazolin-4-yl]pyrrole-2,5-dione (AEB071), a potent and selective inhibitor of protein kinase C isotypes. *J. Med. Chem.* **2009**, *52*, 6193– 6196.

(21) Evenou, J.-P.; Wagner, J.; Zenke, G.; Brinkmann, V.; Wagner. K.; Kovarik, J.; Welzenbach, K.A.; Weitz-Schmidt, G.; Guntermann, C.; Towbin, H.; Cottens, S.;

Kaminski, S.; Letschka, T.; Lutz-Nicoladoni, C.; Gruber, T.; Hermann-Kleiter, N.; Thuille, N.; Baier, G. The potent protein kinase C-selective inhibitor AEB071 (sotrastaurin) represents a new class of immunosuppressive agents affecting early T cell activation. *J. Pharm. Exp. Ther.* **2009**, *330*, 792–801.

(22) Budde, K.; Sommerer, C.; Becker, T.; Asderakis, A.; Pietruck, F.; Grinyo, J. M.; Rigotti, P.; Dantal, J.; Ng, J.; Barten, M. J.; Weber, M. Sotrastaurin, a novel small molecule inhibiting protein kinase C: first clinical results in renal-transplant recipients. *Am. J. Transplant*. **2010**, *10*, 571–581.

(23) Skvara, H.; Dawid, M.; Kleyn, E.; Wolff, B.; Meingassner, J. G.; Knight, H.; Dumortier, T.; Kopp, T.; Fallahi, N.; Stary, G.; Burkhart, C.; Grenet, O.; Wagner, J.; Hijazi, Y.; Morris, R. E.; McGeown, C.; Rordorf, C.; Griffiths, C. E.; Stingl, G.; Jung, T. The PKC inhibitor AEB071 may be a therapeutic option for psoriasis. *J. Clin. Invest*. **2008**, *118*, 3151–3159.

(24) George, D.M.; Breinlinger, E.C.; Friedman, M.; Zhang, Y.; Wang, J.; Argiriadi, M.; Bansal-Parkala, P.; Barth, M.; Duignan, D.B.; Honore, P.; Lang, Q.; Mittelstadt, S.; Potin, D.; Rundell, L.; Edmunds, J. J. Discovery of selective and orally bioavailable protein kinase Cθ (PKCθ) inhibitors from a fragment hit. *J. Med. Chem.* **2015**, *58*, 222-236.

(25) George, D.M.; Breinlinger, E.C.; Argiriadi, M.; Zhang, Y.; Wang, J.; Bansal-Parkala, P.; Duignan, D.B.; Honore, P.; Lang, Q.; Mittelstadt, S.; Rundell, L.; Schwartz, A.; Sun, J; Edmunds, J.J. Optimized protein kinase Cθ (PKCθ) inhibitors reveal only modest anti-inflammatory efficacy in a rodent model of arthritis. *J. Med. Chem.* **2015**, *58*, 333-346.

(26) Jimenez, J.-M.; Davis, C. J.; Boyall, D.; Fraysse, D.; Knegtel, R.; Settimo, L.; Young, S.; Bolton, C.; Chiu, P.; Curnock, A.; Rasmussen, R.; Tanner, A.; Ager, I. Structure-based optimization of aminopyridines as PKCθ inhibitors. *Bioorg. Med. Chem. Lett*. **2012**, *22*, 4645–4649.

(27) Jimenez, J.-M.; Boyall, D.; Brenchley, G.; Collier, P. N.; Davis, C. J.; Fraysse, D.; Keily, S. B.; Henderson, J.; Miller, A.; Pierard, F.; Settimo, L.; Twin, H. C.; Bolton, C. M.; Curnock, A. P.; Chiu, P.; Tanner, A. J.; Young, S. Design and optimization of selective protein kinase Cθ (PKCθ) inhibitors for the treatment of autoimmune diseases. *J. Med. Chem.* **2013**, *56*, 1799–1810.

(28) Curnock, A.; Bolton, C.; Chiu, P.; Doyle, E.; Fraysse, D.; Hesse, M.; Jones, J.; Weber, P.; Jimenez, J.-M. Selective protein kinase Cθ (PKCθ) inhibitors for the treatment of autoimmune diseases. *Biochem. Soc. Trans.* **2014**, *42*, 1524-1528.

(29) Wuitschik, G.; Carreira, E. M.; Wagner, B.; Fischer, H.; Parrilla, I.; Schuler, F.; Rogers-Evans, M.; Müller, K. Oxetanes in Drug Discovery: Structural and Synthetic Insights. *J. Med. Chem*. **2010**, *53*, 3227-3246.

(30) Tzartos, J. S.; Friese, M. A.; Craner, M. J.; Palace, J.; Newcombe, J.; Esiri, M. M.; Fugger, L. Interleukin-17 production in central nervous system-infiltrating T cells and glial cells is associated with active disease in multiple sclerosis. *Am. J. Path*. **2008**, *172*, 146-155.

(31) Lanz, T. V.; Becker, S.; Osswald, M.; Bittner, S.; Schuhmann, M. K.; Opitz, C. A.; Gaikwad, S.; Wiestler, B.Litzenburger, U. M.; Sahm, F.; Ott, M.; Iwantscheff, S.; Grabitz, C.; Mittelbronn, M.; von Deimling, A.; Winkler, F.; Meuth, S. G.; Wick, W.; Platten, M. Protein kinase Cβ as a therapeutic target stabilizing blood-brain barrier disruption in experimental autoimmune encephalomyelitis. *Proc. Natl. Acad. Sci. U. S. A.* **2013**, *110*, 14735-14740.